Article

Title: Maintenance of adaptive dynamics in a bottlenecked range-edge population that retained out-crossing

Authors: Margarita Takou[1], Tuomas Hämälä[2], Evan Koch[3], Kim A. Steige[1], Hannes Dittberner[1], Levi Yant[4], Mathieu Genete[5], Shamil Sunyaev[3], Vincent Castric[5], Xavier Vekemans[5], Outi Savolainen[6], Juliette de Meaux[1]

[1] Institute of Botany, University of Cologne, Cologne, Germany

[2]Department of Plant and Microbial Biology, University of Minnesota, St. Paul, Minnesota, USA.

[3]Department of Biomedical Informatics, Harvard Medical School, Boston, Massachusetts, USA.

[4]School of Life Sciences, University of Nottingham, Nottingham NG7 2RD, UK

[5]Univ. Lille, CNRS, UMR 8198 - Evo-Eco-Paleo, F-59000 Lille, France

[6]Department of Ecology and Genetics, University of Oulu, FIN-90014 Oulu, Finland

Corresponding author: Juliette de Meaux

Corresponding author's email: jdemeaux@uni-koeln.de

Abstract:

During range expansion, edge populations are expected to face increased genetic drift, which in turn can alter and potentially compromise adaptive dynamics, preventing the removal of deleterious mutations and slowing down adaptation. Here, we contrast populations of the European sub-species *Arabidopsis lyrata* ssp *petraea*, which expanded its Northern range after the last glaciation. We document a sharp decline in effective population size in the range-edge population and observe that non-synonymous variants segregate at higher frequencies. We detect a 4.9% excess of derived non-synonymous variants per individual, suggesting an increase of the genomic burden of deleterious mutations in the range-edge population. Inference of fitness effects under the explicit demographic history of each population shows that the range-edge population is depleted in rare deleterious variants, but enriched for fixed ones, resulting in a small net difference in per-individual burden between the range-edge and –core populations. Consistent with this prediction, the range-edge population was not impaired in its growth and survival measured in a common garden experiment. We further observe that the allelic diversity at the self-incompatibility locus, which ensures strict outcrossing, has remained unchanged. Genomic footprints indicative of selective sweeps were broader in the Northern population but not less frequent. This indicates that, despite a dramatic bottleneck and a mild expansion load, adaptive mutations were present in sufficient number to maintain adaptive dynamics at the range-edge of the strictly outcrossing species *Arabidopsis lyrata* ssp. *petraea*.

Keywords: range expansion, adaptation, mutation burden, self-incompatibility locus, negative frequency-dependent selection, selective sweeps

Introduction

Range expansion events, like the postglacial colonization of Northern Europe and Scandinavia from Southern refugia, have had wide influence on the distribution of genetic diversity within species (Hewitt 2000). Through its impact on multiple population genetic processes, range expansion has cascading effects on adaptive dynamics (Excoffier et al. 2009). Indeed, it increases drift (Hallatschek et al. 2007), and leads to both a progressive loss of genetic diversity and increased levels of population differentiation along the expansion route (Austerlitz et al. 1997; Corre and Kremer 1998; Muller et al. 2008; Excoffier et al. 2009; Slatkin and Excoffier 2012). As a consequence, fitness is expected to decrease at the front of the expanding range, causing what is known as the expansion load. The majority of those mutations remain at low frequencies or are lost, but some quickly fix, a phenomenon sometimes termed allele surfing (Klopfstein et al. 2006; Peischl et al. 2013). Although non-synonymous and potentially deleterious mutations are more likely to fix in bottlenecked populations, where the removal of new deleterious mutations is less efficient, it takes some evolutionary time until a significant load accumulates (Lohmueller 2014; Simons et al. 2014; Balick et al. 2015; Do et al. 2015).

Expansion load can interfere with adaptive dynamics. Locally adapted populations that move out of their core range are expected to evolve towards new adaptive peaks (Colautti and Barrett 2013; Savolainen et al. 2013; Wos and Willi 2018). In a population carrying an expansion load, larger adaptive steps might be required to establish a novel range edge, resulting in a slowdown of expansion, especially when dispersal is limiting (Henry et al. 2015). Theoretical studies report complex interactions among parameters such as the strength and heterogeneity of selection, the rate of expansion, as well as the architecture of traits under selection. Expansion rate and adaptive requirements to the newly colonized environments can jointly modulate the fitness decrease observed at the range edge (Gilbert et al. 2017, Gilbert et al. 2018). However, to the best of our knowledge, these predictions remain practically untested in natural populations.

The speed of range expansion can also be limited by species interactions, if these are necessary for reproductive success and survival (Louthan et al. 2015). Many flowering plants rely on insects for pollination and thus fertility (Gibbs 2014). As species expand their range, efficient pollinators can become rare, and a shift towards selfing may help restore reproductive assurance and avoid Allee effects (Jain 1976; Morgan et al. 2005; Gascoigne et al. 2009). Transitions to selfing or mixed- mating systems have often been associated with range expansion (Goodwillie et al. 2005; Levin 2010; Laenen et al. 2018; Baker 1995 but see Cheptou 2012). However, mating system shifts can compromise adaptive processes by exposing populations to inbreeding depression and loss of genetic diversity as they face stress at the margin of their ecological niche (Baker 1995; Slatkin 1995; Ingvarsson 2002; Barrett 2003; Glémin and Ronfort 2013). Yet, increases in the selfing rate can also contribute to the purging of deleterious mutations (Pujol et al. 2009; Glémin and Ronfort 2013; Hadfield et al. 2017; Roessler et al. 2019) and promote the emergence of high fitness individuals at the front range of expansion (Klopfstein et al. 2006). In fact, selfing species generally show the greatest overall range size (Grossenbacher et al. 2015). In this context, plant species that have maintained a strictly outcrossing mating system across their expanded distribution range are particularly intriguing.

The European sub-species *Arabidopsis lyrata ssp. lyrata* has expanded its range Northwards after the last glaciation (Clauss and Koch 2006; Schierup et al. 2006; Koch 2019). Northern populations in *A. l. ssp. petraea* show a strong reduction in diversity (Wright et al. 2003; Muller et al. 2008; Ross-Ibarra et al. 2008; Pyhäjärvi et al. 2012; Mattila et al. 2017). Yet, there is evidence that *A. l. ssp. petraea* populations at the Northern range edge are locally adapted. Reciprocal transplant studies between the Northern and Central European populations showed that Northern populations have the highest survival rate in their location of origin consistent with signals of local adaptation (Leinonen et al. 2009). Major developmental traits such as flowering time, as well as the response to abiotic stress factors, seem to have been targets of natural selection (Sandring et al. 2007; Toivainen et al. 2014; Mattila et al. 2016; Davey et al. 2018; Hämälä and Savolainen 2018). Reciprocal transplant experiments across

four sites in Europe, as well as between populations of different altitude in Norway, indicated that populations at the range margins were locally adapted (Hämälä and Savolainen 2018).

A. lyrata ssp. lyrata enforces self-incompatibility (SI) via the multiallelic S-locus specific to the Brassicaceae family (Bateman 1955; Kusaba et al. 2001). Phylogenetic and genomic analyses of the S-locus have shown that strong negative frequency-dependent selection caused early diversification of the S-locus within the family and a high degree of sharing of S-allele lineages across species (Dwyer et al. 1991; Vekemans et al. 2014). The loss of SI, however, evolved repeatedly in the family (Tsuchimatsu et al. 2012; Vekemans et al. 2014; Durvasula et al. 2017). In fact, some populations of the closely related North American subspecies *A. l. ssp. lyrata*, lost obligate outcrossing at their range margin (Mable et al. 2005; Griffin and Willi 2014; Willi et al. 2018). This transition to selfing has been recently associated with a sharp decrease in average population fitness (Willi et al. 2018). In the sub-species *A. l. ssp. petraea*, instead, SI appears to have been maintained, presumably due to the inbreeding depression, which has been demonstrated using forced selfing (Kärkkäinen et al. 1999; Sletvold et al. 2013).

To gain insight into the combined effects of demographic history and selection processes in an outcrossing range-edge population, we quantified the demographic impact of range expansion in a Northern population of the sub-species *A. l. ssp. petraea* and examined its impact on both negative and positive selection. We compare this population to two populations representative of the core of the species range and specifically ask: i) can we document a decreased efficacy of negative selection in the range-edge population and an increase in the individual burden of deleterious mutations?, ii) does the range-edge population show a decrease in S-allele diversity as expected by an ongoing mating system shift?, and iii) do we detect a slowdown of adaptive dynamics in range-edge *A. l. ssp. petraea* populations ?

We document a strong bottleneck and increased frequency of non-synonymous variants indicative of progressive range expansion. Population genetics analyses, genomic measures and common garden analysis of plant fitness indicate that the bottleneck was too short and not severe enough to allow the accumulation of a significant burden. We further observe that negative frequency-dependent selection on S-alleles has remained efficient and find no evidence that the response to positive selection is impaired in the range-edge population. The outcrossing subspecies *A. l.* ssp *petraea* shows a strong resilience to the effect of range expansion.

Results

Demographic history of three European *A. lyrata ssp. petraea* populations confirms a scenario of range expansion

We analyzed whole genome sequence data for 46 *Arabidopsis lyrata* individuals, of which, 22 were collected in a range edge population in Norway (Spiterstulen, SP), and 17 and 7 individuals from two core populations in Germany (Plech, PL) and Austria (a scattered sample, AUS; Fig 1a), respectively. We first examined the partitioning of genome-wide genetic variation along principle components. The populations of origin were clearly separated on the first two axes. The first principal component (PC) explained 24.95% of the variance, separating the Northern site from the two Central European sites (PL and AUS). The second PC (6.82%) differentiated the AUS and PL sites. AUS individuals were more scattered than SP and PL individuals, presumably because AUS individuals were collected over a broader area (see methods, Fig 1b). Within populations, nucleotide diversity was estimated as the average number of pairwise differences per sites (π) across non-overlapping 10 kb windows. Mean nucleotide diversity of the genomic windows was π=0.0081, π=0.0067 and π = 0.0055 for PL, AUS and SP, respectively (Table S1).

Estimates of pairwise F_{ST} corroborated the Principal Component Analysis (PCA) results. We calculated F_{ST} across 10 kb non-overlapping windows along the genome. Mean F_{ST} was 0.231 (median of 0.232) and 0.234 (median of 0.236) for SP vs. PL or AUS, respectively. Between PL and AUS, differentiation was much lower, with a mean F_{ST} value of 0.079 (median of 0.047). Most of the genetic differentiation resides between Northern and Central European populations and not between PL and AUS, which are geographically closer to each other. Average number of nucleotide differences between pairs of individuals from distinct sites (d_{xy}) confirmed the pattern of inter-population differentiation (Table S1).

Likewise, admixture analysis showed that our samples are best described with K=2 clusters (cross-validation error, cv = 0.397). The SP individuals formed a unique cluster, while PL-AUS individuals grouped together in one cluster. The second most probable scenario (cv = 0.419) was K=3, with each population forming its own cluster (Fig S1).

PCA, F_{ST} and admixture analyses measure genetic differentiation and cannot separate the effects of population history, migration and population size change. We thus used our whole genome dataset to model the demographic history of the three populations with *fastsimcoal2* (Excoffier et al. 2013). In contrast to PCA and F_{ST}, which indicated that PL and AUS are equally distantly related to SP, model selection based on the Akaike information criterion (AIC) indicated that it was significantly more probable that the ancestral population of SP and PL (SP, PL) split from the AUS lineage first (Fig 1c; Table S2). Divergence between (SP, PL) and AUS (T) was estimated to have occurred approximately 292,210 generations ago (CI: 225,574 – 336,016). The split between SP and PL was estimated to have occurred more recently, approximately T = 74,042 generations ago (CI: 51,054 – 100,642). Demographic modelling further indicated that the most probable migration scenario entailed historical migration between all populations (Table S3). The model indicated that gene-flow was higher between

PL and AUS (PL to AUS, $4N_em$ =2.113, (CI: 1.668 – 6.771) and from AUS to PL $4N_em$= 0.039 (CI: 0.05 – 0.125)) than between SP and PL (SP to PL $4N_em$ = 0.038 (CI: 0.013 – 1.699), and PL to SP $4N_em$ = 0.162, (CI: 0.062 – 1.924). Hence, the discrepancy between the observation of moderate population differentiation between PL and AUS despite long historical divergence, is consistent with the maintenance of high gene flow between these Central European populations.

Estimated effective population sizes before and after divergence events indicated bottlenecks in all populations. The size estimate of the ancestral population reached N_e= 839,169 (CI: 823,959 – 877,924). The effective population size (N_e) of SP was reduced approximately 6-fold after it diverged from PL, from N_e= 206,610 (CI: 100,945 – 308,029) to N_e=35,479 (CI: 21,624 – 54,855), respectively before and after the split. In contrast, the PL population experienced a weaker initial bottleneck with N_e reduced by 40% after the split from SP: 127,100 (CI: 87,666 – 162,171). Both SP and PL also experienced more recent population size changes, with a slight increase in SP to a current N_e of 40,886 (23,081 – 47,713), approximately 4,421 (CI: 2,755 – 39,967) generations ago, and a very recent drop in PL to a current N_e of 11,190 (2,573 – 20,751), approximately 143 (CI: 4 – 361) generations ago. The population size in AUS decreased to 219,078 (CI: 148,664 – 249,105) after splitting from an ancestral population shared with PL. We note, however, that the AUS sample consists of individuals collected from three closely located sites, and thus might reflect diversity at a coarser grain than the SP and PL samples.

To test the robustness of bottleneck inference to sample size, we also conducted the demographic modeling with down-sampled data sets (1/3 and 2/3 of SP and PL sample sizes). Even though down-sampling changed the N_e estimates, the fold reductions in population size remained comparable and the bottleneck events are always supported (Table S4). Furthermore, we observed a good correspondence between the observed population-specific SFS (Fig 2a) and those simulated under the best-fit demography model, indicating that the model captures the evolutionary history of these populations reasonably well (data not shown). The demographic modeling therefore confirmed that SP is a range-edge population that can be contrasted to the more range-core populations PL and AUS (Muller et al. 2008; Pyhäjärvi et al. 2012; Mattila et al. 2017). This supports a scenario of colonization in Scandinavia with genetic material from Central European glacial refugia, a history that is common to several plant species (Clauss and Mitchell-Olds 2006; Pyhäjärvi et al. 2007; Ross-Ibarra et al. 2008; Ansell et al. 2010; Schmickl et al. 2010; Pyhäjärvi et al. 2012; Laenen et al. 2018).

We calculated Tajima's D values in 10kb windows for each population (Fig 2b). The distribution of Tajima's D values for SP was shifted towards positive values (mean = 1.230, median = 1.286), which was consistent with the inferred demographic history of a strong recent bottleneck in SP. Tajima's D values for PL and AUS were also mainly positive (mean = 0.313, median 0.265 for PL and mean =0.240, median =0.151 for AUS) but both were significantly lower than in SP (Kolmogorov-Smirnov,

KS test $p < 2.2e-16$ in both cases). The two distributions also differed significantly (KS test $p < 2.2e-16$).

Additionally, analysis of linkage disequilibrium (LD) decay further confirmed the stronger bottleneck experienced by the SP population. LD decay was calculated on the subsample of 12 field collected SP individuals to ensure that native LD levels were analyzed (individuals obtained from crosses in the greenhouse were removed). LD was halved within 2.2 kb in SP, which is considerably slower than for an equally sized sample of PL individuals (LD halved within 0.5kb; Fig 2c).

The distribution of fitness effects

To infer the efficiency of negative selection, we estimated the distribution of fitness effects of new mutations in both core (PL) - and range-edge (SP) populations, taking the demographic history into account (Williamson et al. 2005; Boyko et al. 2008). As the AUS population had a smaller sample size, as well as individuals taken from three different local sites, it was excluded. For SP and PL, we used a modified version of the software fit∂a∂i (Kim et al. 2017). We also fit the 4-fold SFS with a simplified demographic model that excluded AUS and that was compatible with the complex model described above but assumed a larger population size in PL to account for migration from AUS (see Methods). The demographic model showed a very good fit with (putatively neutral) SFS at 4-fold degenerate sites of both PL and SP (Fig S2a-d). Interestingly, this model corresponded very well to the scenario expected for range-core and -margin populations in an expanding species (Fig S2a-b). Distributions of fitness effects of new mutations (DFE) were estimated based on the nonsynonymous (0-fold) folded SFS and taking the demographic history into account. We estimated the shape and scale parameters of a gamma-distributed DFE by fitting the demographic model and the 0-fold SFS of both populations (shape=0.213, scale=552.394, Fig. S2c-d). Using the estimated gamma distribution of effects, we predicted for each frequency bin, the proportion of variants within four bins of selection coefficients (FigS2e-f, Fig. 3a). The strength of s among segregating variants differed between the populations. Neutral and nearly-neutral mutations were found to contribute to a greater proportion of variation in the PL population compared to SP, whereas mutations with a stronger s were found to contribute more to variants segregating in SP (Fig. 3a). Additionally, as a robustness check against our assumed non-synonymous mutation rate and gamma-distributed DFE, we used a multinomial model to predict the DFE fitting only the observed proportions in the folded 0-fold SFS. In this case, the best-fit DFE was a point mass at $2*N_{anc}*s=1.2$, indicating that only slightly deleterious mutations were segregating in the two populations. Although the latter model ignores variation too deleterious to show up in the sample, we found that fixing the proportion of strongly deleterious new mutations to 44% provides a good fit to the observed 0-fold SFS in both populations, indicating that the Ne.s estimate of 1.2 was a reasonable approximation to the strength of selection against mildly deleterious non-synonymous variants (Fig. S2e-f).

Estimates and Measures of accumulated burden in SP individuals

The severe bottleneck in the SP population is expected to have facilitated the fixation of derived variants. Because some of them are expected to be deleterious, we investigated whether the per-individual burden in SP was higher than in PL. The number of derived non-synonymous mutations per Mbp of each lineage has been shown to be an appropriate proxy for the genomic load of a population, because its expectation is unaffected by demographic events (Simons and Sella 2016).

We used the inferred DFE to get an estimate of the expected burden in each of the two populations. PL and SP differed in the frequency of the variants contributing to the burden (Fig. 3b). Low frequency mutations contribute more to the burden in PL. We inferred that an excess of about 10,000 slightly deleterious mutations of frequency below 30% were expected in PL, compared to SP. In the latter, instead, we inferred an almost equal excess of fixed derived mutations in SP. Fixed mutations thus played a more important role in the estimated burden of SP individuals. The net difference, however, was small with an excess burden of 185 mutations per diploid genome in SP, compared to PL (Fig. 3b). Based on 1.2, the point Ne.s estimate for these mutations, and given that the predicted ancestral population size is about 1M, we roughly expect that each of these mutations will have an s of about $1.2.10^{-6}$. If their individual fitness is multiplicative, they will at most contribute a loss of approximately 0.002 % in relative fitness ($1.2.10^{-6}$*185). This loss in fitness through fixation of nearly neutral mutations in the range-edge population is much less than the 3-4% predicted in simulations (Gilbert et al. 2017), suggesting that the bottleneck in the range-margin population SP was not sufficiently long and severe to decrease fitness.

We also directly measured the accumulated burden of deleterious mutations per individual haploid genome in SP and PL by calculating the mean count of derived mutations per haploid genome and corrected by the total number of genotyped sites (see Methods). As expected, the mean per-individual count of derived synonymous mutations did not differ significantly between SP and PL (p = 0.121, Tables S5; Fig S3). There was a shift towards a smaller average number of synonymous mutations per genome in AUS (Fig S3), which likely reflects a residual effect of the overall lower genomic coverage of AUS individuals. Thus, AUS individuals also had to be excluded from this analysis. For each of the other two populations, we estimated the mean count of derived non-synonymous mutations (Fig 3c). The average burden accumulated by SP individuals reached a mean 0.0123 non-synonymous mutation per site (CI: 0.0118 – 0.0127). For PL the mean burden was 0.0117 (CI: 0.0113 – 0.0121), which is 4.9% less than in SP. Permuting individuals among populations revealed that the mean difference between the two populations is significantly different from zero ($p < 10^{-4}$ for SP vs PL). Based on the approximate total of 2M non-synonymous sites per genome, we deduce that there are about 1,200 additional derived non-synonymous mutations per diploid genome in SP individuals, on average, compared to PL. Based on the estimated effect size of deleterious mutations above, this excess would

result in a fitness loss of approximately 1,200 * $1.2.10^{-6}$ = 0.014%. Although this is higher than the theoretical prediction, it is much less than the approximately 3% fitness loss predicted in simulations (Gilbert et al. 2017).

We further used SNPeff (Cingolani et al. 2012) to identify mutations with a high deleterious impact and evaluate whether SP and PL could differ in the number of strongly deleterious mutations. Individuals in SP contained approximately 4.5% more such mutations (0.000164, CI: 0.000148-0.00018) than in PL (0.000156, CI:0.000142-0.000171, Fig 3c; Table S5). This difference was not significant, indicating that the populations did not differ in the proportion of strongly deleterious mutations (p=0.183, Table S5).

SP and PL show similar growth rate in a common garden of the species in the range core.

We further investigated whether a significant fitness erosion could be detected at the phenotypic level in SP. We planted six replicate cuttings of 10 genotypes of each of the two populations in the common garden of University of Cologne. The experiment was initiated early autumn and terminated a year later at the end of the growth season. Although individuals of SP had a comparatively smaller rosette diameter after winter, the rosette diameter as well as their accumulated biomass did not differ from that of PL individuals at the end of the growth season (GLM model, p=0.26, and p=0.28, for the population effects of rosette diameter and accumulated biomass, respectively, Fig S4), due the comparatively higher growth rate of SP individuals during the growth season (Month and Population interaction p < 2.2e-16). It shows that despite its increased per-individual burden and the potential impact of recessive deleterious variants, the cumulative effect of these mutations is not sufficient to impair complex fitness component traits such as growth in the SP population. This observation is in agreement with previous reciprocal transplant experiments involving the same set of *A. lyrata ssp. petraea* populations, which concluded that the SP population is locally adapted (Leinonen et al. 2009). However, it stands in strong contrast with the clear effect of range expansion detected on plant survival and population growth rate in the relative *A. lyrata ssp. lyrata* (Willi et al. 2018).

Potential differences in recessive load in SP and PL

Recessive mutations with deleterious effects can segregate at higher frequency in a bottlenecked population and thus lead to a genomic load in the population that is higher than predicted by measures of per-individual burden (Balick et al. 2015). To evaluate whether recessive deleterious mutations may contribute to the genomic load in SP and PL, we tested whether the F_{IS} distribution of non-synonymous mutations showed a departure from Hardy Weinberg expectations indicative of a selective removal of homozygotes. We found that both in PL and in SP, the F_{IS} distribution of synonymous and non-synonymous mutations was significantly shifted towards lower values, revealing an excess of heterozygous non-synonymous mutations (Fig. 4, KS test p < 2.2e-16). The shift towards negative F_{IS}

values was more pronounced for the high impact variants, which were significantly different from the distribution of the synonymous sites (KS test $p < 2.2e-16$). This pattern suggests that, in both populations, offspring homozygous for deleterious alleles tend to be removed by selection. Compared to PL, the F_{IS} distribution of all sites in SP was shifted towards negative values, indicating a stronger excess of heterozygotes in this population (Fig 4, $p<2.2e-16$). We cannot fully rule out that this effect is not due to mapping inaccuracies, but it was independent from coverage thresholds or SNP density (see Supplementary Material). It therefore suggests that the preferential removal of recessive homozygous might be more important in SP. The per-individual burden we calculated may not fully recapitulate the deleterious load of the populations.

Selective sweeps in the range edge are broader than in the core but equally frequent

We searched for the footprints of selective sweeps within SP and PL – the two populations with the largest sample sizes using the Composite Likelihood Ratio (CLR) test. CLR estimates were computed in windows along the chromosomes with *SweeD* (Pavlidis et al. 2013). Significant deviations from neutral expectation were defined by comparing the observed diversity estimates to neutral diversity estimates simulated under the demographic model obtained above. We used the overlap of outlier CLR and F_{ST} to identify putative selective sweep regions specific to SP or PL (and thus indicative of local selection). We detected signatures of local sweeps within both populations despite their large differences in recent effective population size. In SP, we identified 1,620 local sweep windows, which grouped in 327 genomic regions of average size 7051bp (see methods). Within PL, 745 windows, covering 104 genomic regions (average size 4,384bp), had PL specific signatures for sweep. Hence, the rate of adaptive evolution in the SP populations does not seem to have been compromised by the recent bottleneck.

Genes within the genomic regions carrying a population-specific signature of a selective sweep were extracted and tested for functional enrichment (Supplementary Information). In SP, fifteen Gene Ontology (GO) terms were enriched among genes showing signatures of positive selection (significance based on permutation derived *p* threshold of 0.0295). Interestingly, the top three GO terms were related to plant growth in response to environmental stimuli: “cellular response to iron ion”, “response to mechanical stimulus” and “response to hormone”. This observation is in agreement with the higher growth rate displayed by SP individuals in the common garden experiment. In PL, three GO enriched terms were significant (*p* threshold of 0.02137) and they were “intra-Golgi vesicle-mediated transport”, “regulation of anion transport” and “hexose metabolic process” (Table S6). Some of these functions have been associated with abiotic stress reactions in plants (Howell 2013) and may indicate adaptation in PL to the absence of snow cover protection during the cold season.

We further investigated whether specific groups of candidate genes carried signatures of adaptive evolution. Phenotypic differences in flowering time and especially selection related to the photoperi-

odic pathway, or to development have been shown to contribute to local adaptation in SP (Toivainen et al. 2014; Mattila et al. 2016; Hämälä and Savolainen, 2019), as well as response to abiotic factors such as cold and drought (Vergeer and Kunin 2013; Davey et al. 2018). We thus explored whether specific groups of genes associated with these traits carried signatures of adaptive evolution. We used the *A. thaliana* annotation to identify the *A. lyrata* orthologs of genes involved in these phenotypes. We then tested whether their F_{ST} estimates tended to be higher than the rest of the annotated genes (Table S7). An excess of high F_{ST} values was detected for genes involved in development and light ($p = 0.018$ and $p = 0.036$, respectively). Yet, genes related to dormancy, flowering, cold and water conditions did not exhibit significantly higher F_{ST} values than the control group (Table S7).

Negative frequency-dependent selection maintained S-locus diversity in the range-edge population

Despite a smaller effective population size in SP, strong negative frequency-dependent selection acting on the self-incompatibility locus effectively maintained or restored S-allele diversity. In SP, 15 S-alleles (allelic richness was equal to 7.6) were detected across 22 individuals, with gene diversity at the S-locus equal to 0.828. These values were only slightly lower than to those observed within the 18 PL individuals (14 S-alleles; allelic richness = 8.1; gene diversity = 0.877) and the 7 AUS individuals (10 S-alleles; allelic richness = 10.0; gene diversity = 0.940) (Table 1; Table S8). High S-allele diversity in SP (while a drastic reduction of the diversity at the S-locus would have been expected if a shift in the mating system had occurred), suggests that individuals are highly outcrossing and thus that the past bottleneck does not seem to have affected the mating system. The S-locus F_{ST} between SP and either PL or AUS was equal to 0.027 or 0.037, respectively, values much lower than the whole genome (0.231 or 0.234, respectively) as predicted by Schierup et al. (2001).

Discussion

Genomic burden detectable in range edge population, but no evidence of impaired fitness

The relationship between population size and selection is a centerpiece of population genetics theory. At equilibrium, smaller populations have a lower adaptive potential and increased burden of deleterious alleles (Kimura et al. 1963). These premises formed a viewpoint that population bottlenecks inhibit the removal of deleterious mutations (Kirkpatrick and Jarne 2000; Hamilton 2009; Glémin and Ronfort 2013; Balick et al. 2015). In reality however, it takes time until the equilibrium between gain and loss of mutations is restored in a bottlenecked population, so that population size reduction does not immediately associate with the presence of an increased mutation burden (Simons et al. 2014; Do et al. 2015).

The SP population provides a clear case of a range-edge population likely exposed to a severe bottleneck but with only a mild increase in average burden of deleterious mutations. Demographic model-

ing estimated that the population progressively decreased to about 4.8% of its initial size, despite the population growth estimated in recent generations. In agreement with previous reports (Mattila et al. 2017; Hämälä et al. 2018), this decrease had pronounced population genetics consequences: a markedly lower level of diversity, a slower LD decay and non-synonymous variants segregating at higher frequency. The genome-wide elevation of Tajima's *D* further indicates that the population has not yet returned to equilibrium, since it is still depleted in rare alleles relative to common ones.

Significant mutation load has been associated to post-glacial expansion in several instances, where expansion occurred along with a mating system shift. Individuals of the sister sub-species *A. l. ssp. lyrata* showed a marked increase in phenotypic load at the range edge, particularly in populations that shifted to selfing (Willi et al. 2018). In *Arabis alpina,* individuals sampled in a selfing population of the species Northern European range also appeared to have accumulated a load of deleterious mutations greater than that of populations closer to the range-core (Laenen et al. 2018). Here, we investigated the footprint left by post-glacial range expansion in populations that did not experience a shift in mating system.

To measure the per individual genomic burden of deleterious variation we calculated the number of derived nonsynonymous mutations in individual genomes. This metric has the considerable advantage that it is insensitive to variation in population size (Simons et al. 2014; Do et al. 2015). Other metrics, such as those which use the proportion of variation that is nonsynonymous are confounded by demographic history (Do et al. 2015; Brandvain and Wright 2016; Simons and Sella 2016; Koch and Novembre 2017).

In the range-edge population of *A. lyrata*, prediction based on the estimated DFE indicated that the differences in the demographic histories of the two populations had a strong effect on the frequency of the mutations contributing to the per-individual burden. In SP, fixed mutations contributed comparatively more to the individual per-genome burden, whereas in PL, it was sustained by a greater number of low frequency mutations (Fig. 3b). Overall, our model predicted only an average excess of 185 non-synonymous mutations per diploid genome in SP. This prediction was within an order of magnitude of the excess nonsynonymous burden of about 1,200 observed in the data. The predicted burden may be less that the observed for a number of reasons. It is possible that the SP population experienced a greater number of adaptive substitutions when expanding its range into a new environment. Along this line, we also did not account for the effects of linked selection which could lead to a faster burden accumulation under some scenarios (Marsden et al. 2016). Finally, if we overcorrected for the reduced power to call variants in SP, a consequence of the somewhat lower coverage of whole genome sequences in this population in our dataset, we would have underestimated the population bottleneck, which would also lead to an underestimate of the burden.

This number of deleterious mutations per individual genome, however, remains a crude estimator. First, it underestimates the impact of recessive deleterious mutations (Balick et al. 2015). The strong deficit of homozygous large effect mutations within SP and PL clearly shows that recessive deleterious variants do contribute to the load in these populations, especially within SP in which mutations of strong deleterious effect tended to segregate at higher frequency (Fig. 3a). Second, indirect methods may be more powerful. For example, patterns of Neanderthal introgression in the modern human genome, revealed the increased deleterious load of the introgressing genome and its preferential removal in the larger *Homo sapiens* population (Juric et al. 2016). In maize, an outcrossing crop, which experienced two successive drastic bottlenecks during domestication, the variance in gene expression revealed a burden of deleterious regulatory mutations that significantly impaired fitness (Kremling et al. 2018).

The accumulated effect of deleterious mutations in the genome is expected to negatively impact any polygenic fitness trait, such as e.g. growth rate in plants (Leinonen et al. 2009; Debieu et al. 2013; Younginger et al. 2017). Our analysis indicated that the predicted effect of deleterious mutations is around $1.2.10^{-6}$ and therefore too small to lead to a detectable decrease in fitness. The lack of growth and survival difference observed in common gardens within the range-core area of the species both here and in a previous study, also support the notion that SP individuals do not suffer from a massive deleterious burden (Fig S4, Leinonen et al. 2009). Our results therefore indicate that in this plant system, the severity and duration of the bottleneck experienced at the range-edge was not sufficient to allow the emergence of an impactful load of deleterious mutations. In this sense, the accumulated deleterious burden in SP is more similar to the consequences of the out-of-Africa bottleneck in humans, which has had substantial effects on the SFS of deleterious variation, but no detectable effect on the genetic load (Simons et al. 2014; Do et al. 2015).

Evidence for effective negative-frequency dependent selection

Small size populations are also expected to require larger effect mutations to respond to selection (Hamilton 2009). This, however, does not impair the response to negative frequency-dependent selection on S-allele, and the maintenance of an effective level of outcrossing. The S-locus diversity, both in terms of allelic richness and heterozygosity, was found to be only marginally lower in SP compared to PL and AUS. Similar levels of S-allele diversity were also reported for 12 Icelandic *A. lyrata* ssp *petraea* populations (Schierup et al. 2008), that share recent history with SP (Pyhäjärvi et al. 2012). This, together with the observation that homozygote genotypes (and thus crypting selfing events) are not more frequent throughout the genome, confirms that SP has maintained a functional self-incompatibility system, despite the historical genetic bottleneck. The persistence of obligate outcrossing in Scandinavian *A. l.* ssp. *petraea* populations has previously been discussed by Sletvold et al. (2013), who attributed the maintenance of a functional self-incompatibility system to the strong in-

breeding depression levels occurring in those populations. In contrast, low inbreeding depression in North American populations of *A. lyrata* ssp. *lyrata* may have been a key feature that contributed to independent breakdown of self-incompatibility associated with bottlenecks at the species distribution edges (Willi et al. 2013; Willi et al. 2018). Comparable to the North American populations of *A.l. ssp lyrata*, many other examples of loss of self-incompatibility have been reported after range expansion or strong genetic bottlenecks. For example, Scandinavian populations of *Arabis alpina* (Laenen et al. 2018), in disjunct marginal populations of race a4 in *Leavenworthia alabamica* (Busch et al. 2011), and in the form of a strong bottleneck associated with loss of self-incompatibility and speciation in *Capsella rubella* (Guo et al. 2009). Our result also illustrates the remarkable power of negative frequency-dependent selection acting on the S-locus at promoting a high level of resilience against the effect of a bottleneck on allelic diversity. Similar results were found in *L. alabamica*, were the authors did not find reduced S-allele diversity or mate limitation in outcrossing populations from small patches as compared to large populations (Busch 2005). Even if allelic diversity could have been reduced at the time of bottleneck in Scandinavian populations of *A. lyrata*, theory predicts that negative frequency-dependent selection promotes higher effective migration rates at the S-locus as compared to control loci (Schierup 1998), suggesting that high allelic diversity could have also been restored subsequently by gene flow.

Adaptive dynamics maintained in SP

Small size populations are also expected to require larger effect mutations to adapt, although these mutations are rare (Hamilton 2009). Whether a population size reduction immediately reduces adaptive evolution is, however, a complex question in the context of range expansion (Gilbert et al. 2017). If populations have to adapt locally at the range edge, the rate of geographical expansion slows down, along with the severity of the expansion bottleneck (Gilbert et al. 2017). A decrease in population size, however, increases the range of beneficial alleles that behave effectively neutrally (Lynch 2007). Searching for signals of selective sweeps in SP, after accounting for its demography, we identified 327 regions that formed outlier for both CLR and F_{ST} statistics. In fact, the number of genomic regions displaying a signature of positive selection was greater in SP than in PL, a pattern that has been observed also in Northern Swedish populations of *A. thaliana* in contrast to Southern Swedish populations (Huber et al. 2014). However, we cannot exclude that some of the signal detected in SP could also result from the surfing of new alleles towards the range margin, which can mimic signatures of adaptive evolution and create false positive signatures of adaptation (Excoffier et al. 2009). Functional enrichments among regions displaying signatures of local positive selection, however, indicate the presence of true positive signals. Within those regions, functions involved in the response to stress were enriched, in agreement with a previous study investigating micro-geographical patterns of local adaptation in Norwegian populations connected by gene flow (Hämälä et al. 2018; Hämälä and Savolainen 2019). We also found a significant enrichment in genes involved in light perception, a function

enriched in loci differentiating the SP population from a close-by population of lower elevation (Hämälä and Savolainen 2019). Furthermore, the F_{ST} distribution of genes related to development was significantly shifted towards higher values, suggesting polygenic selection on alleles associated to this function (Foll et al. 2014; Daub et al. 2015; Stephan 2016). Previous work has documented that Scandinavian populations display differences in several traits related to growth and resource allocation, including plant size, inflorescence production and fruit production (Quilot-Turion et al. 2013; Hämälä et al. 2018). Both local and regional reciprocal transplant experiments have revealed local adaptation in this species (Leinonen et al. 2009; Hämälä et al. 2018). This shows that adaptive dynamics are ongoing also at smaller geographical scale in this system and is consistent with the broad genomic signals of positive selection we observed.

Conclusions

Signatures of positive selection in the genome of SP indicate that it has a history of adaptive evolution that is comparable to that observed in PL. The maintenance of strict outcrossing in *A. l. ssp. petraea*, probably mitigated the effect of the expansion bottleneck and sustained adaptive evolution compared to populations which evolved selfing during range expansions (Charlesworth et al. 1979). Taken together, our analyses show that range-edge populations of the European *A. l. ssp. petraea* and its associated decrease in population size did not alter adaptive dynamics, presumably thanks to the maintenance of both outcrossing and gene flow (Gilbert et al. 2017; Hämälä and Savolainen 2019).

Materials and Methods

Plant Material, Sequencing and Data Preparation

Genomic sequences of *A. l. ssp. petraea* populations of 22 individuals originating from Spiterstulen in Norway (SP; 61.41N, 8.25E), 17 individuals originating from Plech in Germany (PL; 49.65N, 11.45E) and a scattered sample of 7 individuals from Austria (AUS; 47.54N, 15.58E; 47.55N, 15.59E; 47.58N, 16.9E) were used in the analysis (Fig 1a). Details on the sequencing methodology is given in Supplementary Information.

Analysis of population structure

Genetic diversity and differentiation along the chromosomes were calculated with PopGenome package (Pfeifer et al. 2014) in the R environment version 3.4.4 (R Core Team 2018). Specifically, we calculated pairwise nucleotide fixation index (F_{ST}), nucleotide diversity between (d_{xy}) and within population (π) in 10kb non overlapping windows for each chromosome with functions F_ST.stats, diversity.stats.between and diversity.stats.within, respectively (Wakeley 1996; Hudson and Wayne, 1992). In order to avoid biased F_{ST} estimates (Cruickshank and Hahn 2014), the windows that had F_{ST} above 0.8, dxy and π below 0.001 in at least one population comparison, were removed from the analysis.

Tajima's D was calculated with the function neutrality.stats of PopGenome. The linkage disequilibrium for the field collected SP and PL individuals was calculated along the genome with the default functions of PopLDdecay (Zhang et al. 2019) and the values were plotted in R.

Principal component analysis (PCA) of the genomic data was conducted with adegenet package (Jombart 2008) using a dataset including only every 300th SNP to reduce computational load. This reduced dataset of 233,075 SNPs was also used to calculate SNP based F_{IS} for each population with Hierfstat (Goudet 2005) package function basic.stats (Alexander et al. 2009; Goudet and Jombart 2015). The F_{IS} value of each gene was estimated based on the median F_{IS} value of its SNPs, for SP and PL.

For the admixture analysis (Alexander et al. 2009) bed files were generated with PLINK (Purcell et al. 2007), which were then analyzed for clusters K=1 till K=5, with 10 iterations of cross-validation each. The clusters were normalized across runs using CLUMPAK (Kopelman et al. 2015) and subsequently they were plotted in R.

Demography simulations

To study the demographic history of these populations, we conducted site frequency spectra (SFS) based coalescent simulations with fastsimcoal2 v2.6.0.3 (Excoffier et al. 2013). Folded 3D SFS, comprising of SP, PL and AUS individuals, was estimated from 4-fold sites with ANGSD v0.917 (Korneliussen et al. 2014), using the same filtering steps as with variant calls. We first considered models with all possible divergence orders (see Table S2), and then compared models with five different migration scenarios, guided by previous work on the SP and PL populations (Mattila et al. 2017, Hämälä et al. 2018): no migration, current migration between PL and AUS, historic migration between PL and AUS, and historic migration between all three populations (Table S3). Each model was repeated 50 times and ones with the highest likelihoods used for model selection was based on Akaike information criterion (AIC) scores. Confidence intervals were estimated by fitting the supported model to 100 nonparametric bootstrap SFS. We used these models to define effective populations sizes (N_e), divergence times (T) and migration rates (m). To evaluate how the estimated demography influences measures of positive selection, we used the N_e, T and m parameters in combination with recombination rate estimates derived from an *A. lyrata* linkage map (Hämälä et al. 2017) to generate 10,000 10 kb fragments with *ms* (Hudson 2002). These data were then used to define neutral expectations for analysis of positive selection.

Estimating the distribution of fitness effects

For analyzing the strength of selection, vcf files were first re-filtered for each population separately, as described in the section "data preparation". This was done to retain positions that only needed to be

removed in one population. Sites with data for more than 80% of the individuals were randomly down sampled so that each position had the same number of alleles. Because the SP and PL populations differed in the number of individuals sampled, individuals in the SP population were further randomly down-sampled at each position to give the same number of alleles in both populations. The folded site frequency spectrum was determined for each population. Details on the pipeline are given in Supplementary Information.

A modified version of the program fit∂a∂i (Kim et al. 2017) was used to estimate the distribution of fitness effects. This extension to the ∂a∂i program (Gutenkunst et al. 2009), which infers demographic history as well as selection based on genomic data, allows us to specify the demographic model when inferring selection. Because we only fit the DFE to variation in PL and SP, we first fit a simplified demographic model for these populations only (Fig S2a-b). The simplified demographic model was inferred by maximizing the composite likelihood of the folded SFS at 4-fold degenerate sites in PL and SP using the "L-BFGS-B" method and basinhopping algorithm implemented in scipy. These models provided a good fit of the predicted neutral SFS to the data (Fig S2c-d). They were compatible with the complex 3-population model, but assumed a larger ancestral population size to account for migration from AUS. This model also indicated that the increase in population size following the last bottleneck may have been underestimated in SP (Fig 3c). The estimated 4-fold population scaled mutation rate theta reached 24,000 for PL. It was multiplied by 2.76 to get the 0-fold mutation rate, i.e. the non-synonymous mutation rate for PL. In all instances, the theta used for the SP population had to be constrained to $theta_{PL}$*0.74, to account for the difference in number of retained sites after all filters differed between the populations.

The 0-fold SFS and the demographic model were then used to fit the DFE by estimating the shape and scale parameter of a gamma distribution of selection coefficients. We used both a multinomial model (without using the population scaled mutation rate, theta) and a Poisson model (including theta) to estimate the DFE. The primary difference between these models is that the multinomial model only fits the DFE for variation sufficiently weakly selected to be observed in the sample. The reason for this is that the multinomial model only fits the proportions of alleles observed at different frequencies (the "shape" of the SFS) and does not consider the decrease in per-site reduction in variation compared to 4-fold sites. Strongly deleterious variation will largely be absent from our moderate sample size and therefore does not affect the shape of the SFS. In practice we found that the gamma DFE fit using the multinomial method converged on a point mass at a single selection coefficient. After the DFE for observed variation was fit using the multinomial approach, we also estimated the fraction of strongly deleterious mutations by examining the ratio of the observed SFS to that under the multinomial DFE using the theta calculated for 0-fold sites. This ratio gives an estimate of the fraction of mutations that are sufficiently weakly selected to be observed in the sample.

Although fit∂a∂i includes a function for finding the maximum likelihood values for DFE parameters, we had to implement a different function because we were fitting the parameters to the composite likelihood of the SFS in both populations. We used functions in ∂a∂i to calculate the likelihood and found maximum likelihood parameters using Sequential Least Squares Programming as implemented in scipy.

The DFE describes the distribution of fitness effects of new mutations arising in a population, and as such is independent of the demographic history. It was therefore assumed to be the same in both populations. To predict properties of genetic variation in the two populations, we calculated the distribution of selection coefficients for variants in each count of the SFS by applying Bayes' rule to the expected SFS under each selection coefficient and the distribution of s based on the gamma distribution of the DFE estimated using the Poisson model. Scripts are available upon request.

Genomic burden estimates

We estimated the difference in burden between the populations by first calculating the expected joint SFS for PL and SP under the selection coefficient fit by the multinomial model, using the theta value for PL as this population had the greater power in calling SNPs. For each entry in the SFS we then calculated the difference in the expected count between PL and SP, weighted by their frequency in the sample to account for their probability of being present in an individual genome. Crucially, we also counted alleles that were fixed in one population but not the other. The cumulative difference over all frequencies gives the overall expected difference in the derived allele burden (Scripts are available as supplementary information). Additionally, we used the number of derived non-synonymous mutations per individual to quantify the population's genomic burden (Simons and Sella, 2016). We used SNPeff (Cingolani et al. 2012) to annotate synonymous and non-synonymous sites, as well as sites with different level of high putative impact on the protein, whose ancestral state inference was done comparing to *A.thaliana* and *C.rubella* (see Supplementary Material). Then we counted their respective numbers per individual, with weight of +1 for each instance of homozygous state of the derived allele and as +0.5 for the heterozygous sites. We divided the counts by the total number of genotyped sites, in order to correct for differences in genome mapping between the individuals. The genomic load of each population was calculated as the mean of the weighted number of non-synonymous sites of individual samples. The synonymous sites were used to confirm the robustness of the analysis, as they are expected to not differ among the populations. The confidence intervals for each population, were estimated by bootstrapping with replacement of 1Mbp windows to simulate each time a whole genome (207 1Mb regions). Significance of the mean load difference between SP and PL was estimated following Simon and Sella (2016). Briefly we bootstrapped 16 1Mbp-windows of the genome with replacement and selected two random samples from the union of the two populations to create two groups of size equal to the original populations. This generated a random distribution of expected

variance in the mean derived mutation counts. We used the quantile of this distribution to determine the *p* value.

Comparative analysis of growth rate and biomass accumulation in a common garden experiment

We propagated clonally 10 genotypes from SP and 10 from PL to study growth in a common garden setting. The experiment was initiated in September 2017 and ended August 2018 and took place at the garden of the University of Cologne. Throughout the growing season (March to August) we scored monthly diameter size, in millimeters, as a proxy for vegetative growth. At the end of the growing season, we harvested the above ground material to estimate the dry to fresh weight ratio of the plants as a proxy for the plants' biomass. The phenotypic data are provided in Table S11. Differences between the two populations were tested in R with linear mixed models using the library lme4 (Bates et al. 2015). The model included population and month of the measurement taken as fixed effects. The genotype and replicate number were included as random effects in order to correct for pseudoreplication resulting from sampling the same individuals multiple times throughout the experiment. Significance levels were estimated with a type-II likelihood-ratio-test using the function Anova, from car library (Fox and Weisberg 2019).

Scan for selective sweeps

Areas influenced by selective sweeps were inferred by estimating composite likelihood ratios with SweeD v4.0 (Pavlidis et al. 2013). The analysis was done in 2 kb grid sizes for the SP and PL samples. As a bottleneck can easily bias CLR estimates (Jensen et al. 2007), we used data simulated under the best supported demographic model to define limits to neutral variation among the observed estimates. Estimates exceeding the 99th percentile of neutral CLR values were considered putatively adaptive. We combined significant grid points within 10 kb regions to create outlier windows. Grid points that had no other outliers within 10 kb distance were removed from the analysis. Next, we examined the sweep regions in combination with regions showing elevated differentiation to find areas targeted by strong selection after the populations diverged. As with CLR, windows with F_{ST} values above the 99th percentile of their distribution were considered outliers. Genes from the regions showing higher than neutral differentiation with both CLR and F_{ST} were extracted. Gene Ontology enrichment analysis was performed in R with the topGO package (Subramanian et al. 2005; Alexa and Rahnenfuhrer 2016). Significance of the enrichment was evaluated with Fisher's exact test. Significance threshold was evaluated by permutating the sample's population identity 1,000 times.

Identification of S alleles

We genotyped individuals at the self-incompatibility locus (S-locus) with a genotyping pipeline (Genete et al. 2019) using raw Illumina reads from each individual and a database of all available sequences of *SRK* (the self-incompatibility gene expressed in the pistil) from *A. lyrata*, *A. halleri* and *Capsella grandiflora* (source: GenBank and unpublished sequences). Briefly, this pipeline uses Bowtie2 to align raw reads against each reference sequence from the database and produces summary statistics with Samtools (v1.4) allowing to identify alleles at the S-locus (S-alleles). Coverage statistics allow to reliably identify homozygote versus heterozygote individuals at the S-locus. Genotype data was used to compute population genetic statistics using Fstat (Goudet 1995): number of alleles per sample, sample allelic richness (a standardized estimate of the number of alleles taking into account differences in sample sizes among populations, computed after the rarefaction method described in El Mousadik and Petit 1996, gene diversity (expected heterozygosity under Hardy-Weinberg hypotheses), and F_{ST} (unbiased estimate of the among population fixation index).

Identification of gene functional groups

F_{ST}, dxy and π were estimated for all genes according to the *A. lyrata* gene annotation version 1.0.37 with PopGenome and as described above for the genomic windows. Genes that had functions involved in light, cold, flowering, plant development and dormancy were determined based on the gene ontology of the sister species *A. thaliana.* To explore whether the aforementioned groups of genes had genetic differentiation estimates that were significantly different from the genome-wide background, we performed a non-parametric, two sample Kolmogorov Smirnov test (Marsaglia et al. 2003) between the gene group of interest and the rest of the genomic genes identified in *A. thaliana* and belong in a GO group (ks.test function in R).

Data Availability

All sequence data are available in either NCBI Short Read Archive (SRA; https://www.ncbi.nlm.nih.gov/sra) or in the European Nucleotide Archive (ENA; https://www.ebi.ac.uk/ena) with accession codes: SAMN06141173-SAMN06141198 (SRA; Mattila et al. 2017), SRP144592 (SRA; Hämälä et al. 2018), PRJEB34247(ENA; Marburger et al. 2019), and PRJNAXXXXX (ENA; whole genome sequences generated for this project and the rest of PL sequences).

Acknowledgements

We thank M. Nothnagel, B. Wieters, and G. Schmitz for insightful discussions and comments on the results; M.Nordborg and P.Novikova for PL sequences; B. Laenen for help with the DFE data preparation; V. Kovacova for help with inference of derived and ancestral alleles; K. Bell for lab assistance; students and gardeners at the university of Cologne for assisting with the field experiment; and Co-

logne Center for Genomics (Now West Germany Center) for sequencing of SP samples. This project was funded by ERC projects #648617 Adaptoscope, #648321 (Novel) and Horizon 2020 research and innovation programme [grant number ERC-StG 679056 HOTSPOT], via a grant to L.Y.. The authors also thank the Région Hauts-de-France, the Ministère de l'Enseignement Supérieur et de la Recherche (CPER Climibio), the Biocenter Oulu and the European Fund for Regional Economic Development for their financial support.

References

Alexander DH, Novembre J, Lange K. 2009. Fast model-based estimation of ancestry in unrelated individuals. Genome Res. 19:1655–1664.

Ansell SW, Stenøien HK, Grundmann M, Schneider H, Hemp A, Bauer N, Russell SJ, Vogel JC. 2010. Population structure and historical biogeography of European Arabidopsis lyrata. Heredity 105:543–553.

Austerlitz F, Jung-Muller B, Godelle B, Gouyon P-H. 1997. Evolution of Coalescence Times, Genetic Diversity and Structure during Colonization.

Baker HG. 1995. Self-Compatibility and Establishment After "Long-Distance" Dispersal. 9:347–349.

Balick DJ, Do R, Cassa CA, Reich D, Sunyaev SR. 2015. Dominance of Deleterious Alleles Controls the Response to a Population Bottleneck. PLOS Genetics 11:e1005436.

Barrett SCH. 2003. Mating strategies in flowering plants: the outcrossing–selfing paradigm and beyond.Dickinson HG, Hiscock SJ, Crane PR, editors. Philosophical Transactions of the Royal Society of London. Series B: Biological Sciences 358:991–1004.

Bateman AJ. 1955. Self-incompatibility systems in angiosperms: III. Cruciferae. Heredity 9:53–68.

Bates D, Mächler M, Bolker B, Walker S. 2015. Fitting Linear Mixed-Effects Models Using lme4. Journal of Statistical Software 67:1–48.

Busch JW. 2005. The evolution of self-compatibility in geographically peripheral populations of Leavenworthia alabamica (Brassicaceae). American Journal of Botany 92:1503–1512.

Busch JW, Joly S, Schoen DJ. 2011. Demographic Signatures Accompanying the Evolution of Selfing in Leavenworthia alabamica. Molecular Biology and Evolution 28:1717–1729.

Charlesworth Deborah, Charlesworth Brian, Maynard Smith J., Holliday Robin. 1979. The evolutionary genetics of sexual systems in flowering plants. Proceedings of the Royal Society of London. Series B. Biological Sciences 205:513–530.

Cheptou P-O. 2012. Clarifying Baker's Law. Ann Bot 109:633–641.

Cingolani P, Platts A, Wang LL, Coon M, Nguyen T, Wang L, Land SJ, Lu X, Ruden DM. 2012. A program for annotating and predicting the effects of single nucleotide polymorphisms, SnpEff. Fly (Austin) 6:80–92.

Clauss MJ, Koch MA. 2006. Poorly known relatives of Arabidopsis thaliana. Trends in Plant Science 11:449–459.

Clauss MJ, Mitchell-Olds T. 2006. Population genetic structure of Arabidopsis lyrata in Europe. Molecular Ecology 15:2753–2766.

Colautti RI, Barrett SCH. 2013. Rapid Adaptation to Climate Facilitates Range Expansion of an Invasive Plant. Science 342:364–366.

Corre VL, Kremer A. 1998. Cumulative effects of founding events during colonisation on genetic diversity and differentiation in an island and stepping-stone model. Journal of Evolutionary Biology 11:495–512.

Cruickshank TE, Hahn MW. 2014. Reanalysis suggests that genomic islands of speciation are due to reduced diversity, not reduced gene flow. Mol Ecol 23:3133–3157.

Daub JT, Dupanloup I, Robinson-Rechavi M, Excoffier L. 2015. Inference of Evolutionary Forces Acting on Human Biological Pathways. Genome Biology and Evolution 7:1546–1558.

Davey MP, Palmer BG, Armitage E, Vergeer P, Kunin WE, Woodward FI, Quick WP. 2018. Natural variation in tolerance to sub-zero temperatures among populations of Arabidopsis lyrata ssp. petraea. BMC Plant Biology 18:277.

Debieu M, Tang C, Stich B, Sikosek T, Effgen S, Josephs E, Schmitt J, Nordborg M, Koornneef M, de Meaux J. 2013. Co-Variation between Seed Dormancy, Growth Rate and Flowering Time Changes with Latitude in Arabidopsis thaliana. PLOS ONE 8:e61075.

Do R, Balick D, Li H, Adzhubei I, Sunyaev S, Reich D. 2015. No evidence that selection has been less effective at removing deleterious mutations in Europeans than in Africans. Nature Genetics 47:126–131.

Durvasula A, Fulgione A, Gutaker RM, Alacakaptan SI, Flood PJ, Neto C, Tsuchimatsu T, Burbano HA, Picó FX, Alonso-Blanco C, et al. 2017. African genomes illuminate the early history and transition to selfing in Arabidopsis thaliana. PNAS 114:5213–5218.

Dwyer KG, Balent MA, Nasrallah JB, Nasrallah ME. 1991. DNA sequences of self-incompatibility genes from Brassica campestris and B. oleracea: polymorphism predating speciation. Plant Mol Biol 16:481–486.

El Mousadik A, Petit RJ. 1996. High level of genetic differentiation for allelic richness among populations of the argan tree [Argania spinosa (L.) Skeels] endemic to Morocco. Theoret. Appl. Genetics 92:832–839.

Excoffier L, Dupanloup I, Huerta-Sánchez E, Sousa VC, Foll M. 2013. Robust Demographic Inference from Genomic and SNP Data.Akey JM, editor. PLoS Genet 9:e1003905.

Excoffier L, Foll M, Petit RJ. 2009. Genetic Consequences of Range Expansions. Annual Review of Ecology, Evolution, and Systematics 40:481–501.

Foll M, Gaggiotti OE, Daub JT, Vatsiou A, Excoffier L. 2014. Widespread Signals of Convergent Adaptation to High Altitude in Asia and America. The American Journal of Human Genetics 95:394–407.

Fox J, Weisberg S. 2019. An R Companion to Applied Regression. Third. Sage Available from: https://socialsciences.mcmaster.ca/jfox/Books/Companion/

Gascoigne J, Berec L, Gregory S, Courchamp F. 2009. Dangerously few liaisons: a review of mate-finding Allee effects. Population Ecology 51:355–372.

Genete M, Castric V, Vekemans X. 2019. Genotyping and de novo discovery of allelic variants at the Brassicaceae self-incompatibility locus from short read sequencing data. Mol Biol Evol 37:1193-1201

Gibbs PE. 2014. Late-acting self-incompatibility – the pariah breeding system in flowering plants. New Phytologist 203:717–734.

Gilbert KJ, Peischl S, Excoffier L. 2018. Mutation load dynamics during environmentally-driven range shifts.Bomblies K, editor. PLOS Genetics 14:e1007450.

Gilbert KJ, Sharp NP, Angert AL, Conte GL, Draghi JA, Guillaume F, Hargreaves AL, Matthey-Doret R, Whitlock MC. 2017. Local Adaptation Interacts with Expansion Load during Range Expansion: Maladaptation Reduces Expansion Load. The American Naturalist 189:368–380.

Glémin S, Ronfort J. 2013. Adaptation and Maladaptation in Selfing and Outcrossing Species: New Mutations Versus Standing Variation. Evolution 67:225–240.

Goodwillie C, Kalisz S, Eckert CG. 2005. The Evolutionary Enigma of Mixed Mating Systems in Plants: Occurrence, Theoretical Explanations, and Empirical Evidence. Annual Review of Ecology, Evolution, and Systematics 36:47–79.

Goudet J. 1995. FSTAT (Version 1.2): A Computer Program to Calculate F-Statistics. Journal of Heredity 86:485–486.

Goudet J. 2005. hierfstat, a package for r to compute and test hierarchical F-statistics. Molecular Ecology Notes 5:184–186.

Goudet J, Jombart T. 2015. hierfstat: Estimation and Tests of Hierarchical F-statistics. R package version 0.04-22. Available from: https://CRAN.R-project.org/package=hierfstat

Griffin PC, Willi Y. 2014. Evolutionary shifts to self-fertilisation restricted to geographic range margins in North American Arabidopsis lyrata. Ecology Letters 17:484–490.

Grossenbacher D, Runquist RB, Goldberg EE, Brandvain Y. 2015. Geographic range size is predicted by plant mating system. Ecology Letters 18:706–713.

Guo Y-L, Bechsgaard JS, Slotte T, Neuffer B, Lascoux M, Weigel D, Schierup MH. 2009. Recent speciation of Capsella rubella from Capsella grandiflora, associated with loss of self-incompatibility and an extreme bottleneck. Proceedings of the National Academy of Sciences 106:5246–5251.

Gutenkunst RN, Hernandez RD, Williamson SH, Bustamante CD. 2009. Inferring the Joint Demographic History of Multiple Populations from Multidimensional SNP Frequency Data. PLOS Genetics 5:e1000695.

Hadfield J, Harris SR, Seth-Smith HMB, Parmar S, Andersson P, Giffard PM, Schachter J, Moncada J, Ellison L, Vaulet MLG, et al. 2017. Comprehensive global genome dynamics of Chlamydia trachomatis show ancient diversification followed by contemporary mixing and recent lineage expansion. Genome Res 27:1220–1229.

Hallatschek O, Hersen P, Ramanathan S, Nelson DR. 2007. Genetic drift at expanding frontiers promotes gene segregation. Proceedings of the National Academy of Sciences 104:19926–19930.

Hämälä T, Mattila TM, Leinonen PH, Kuittinen H, Savolainen O. 2017. Role of seed germination in adaptation and reproductive isolation in Arabidopsis lyrata. Molecular Ecology 26:3484–3496.

Hämälä T, Mattila TM, Savolainen O. 2018. Local adaptation and ecological differentiation under selection, migration, and drift in Arabidopsis lyrata. Evolution 72:1373–1386.

Hämälä T, Savolainen O. 2019. Genomic patterns of local adaptation under gene flow in Arabidopsis lyrata. Molecular Biology and Evolution 36:2557–2571.

Hamilton MB. 2009. Population Genetics. Chichester, UK; Hoboken, NJ: Wiley-Blackwell

Henry RC, Barto KA, Travis JMJ. 2015. Mutation accumulation and the formation of range limits. Biology Letters 11:20140871–20140871.

Hewitt G. 2000. The genetic legacy of the Quaternary ice ages. Nature 405:907–913.

Hohmann N, Wolf EM, Lysak MA, Koch MA. 2015. A Time-Calibrated Road Map of Brassicaceae Species Radiation and Evolutionary History. The Plant Cell:tpc.15.00482.

Howell SH. 2013. Endoplasmic reticulum stress responses in plants. Annual review of plant biology 64:477–499.

Huber CD, Nordborg M, Hermisson J, Hellmann I. 2014. Keeping It Local: Evidence for Positive Selection in Swedish Arabidopsis thaliana. Mol Biol Evol 31:3026–3039.

Hudson RR. 2002. Generating samples under a Wright-Fisher neutral model of genetic variation. Bioinformatics 18:337–338.

Hudson RR, Wayne MS. 1992. Estimation of Levels of Gene Flow From DNA Sequence Data. 132:583–589.

Ingvarsson P. 2002. A Metapopulation Perspective on Genetic Diversity and Differentiation in Partially Self-Fertilizing Plants. Evolution 56:2368–2373.

Jain SK. 1976. The Evolution of Inbreeding in Plants. Annual Review of Ecology and Systematics 7:469–495.

Jensen JD, Thornton KR, Bustamante CD, Aquadro CF. 2007. On the Utility of Linkage Disequilibrium as a Statistic for Identifying Targets of Positive Selection in Nonequilibrium Populations. Genetics 176:2371–2379.

Jombart T. 2008. adegenet: a R package for the multivariate analysis of genetic markers. Bioinformatics 24:1403–1405.

Juric I, Aeschbacher S, Coop G. 2016. The Strength of Selection against Neanderthal Introgression. PLOS Genetics 12:e1006340.

Kärkkäinen K, Kuittinen H, Treuren R van, Vogl C, Oikarinen S, Savolainen O. 1999. Genetic Basis of Inbreeding Depression in Arabis Petraea. Evolution 53:1354–1365.

Kim BY, Huber CD, Lohmueller KE. 2017. Inference of the Distribution of Selection Coefficients for New Nonsynonymous Mutations Using Large Samples. Genetics 206:345–361.

Kimura M, Maruyama T, Crow JF. 1963. The Mutation Load in Small Populations. Genetics 48:1303–1312.

Klopfstein S, Currat M, Excoffier L. 2006. The Fate of Mutations Surfing on the Wave of a Range Expansion. Molecular Biology and Evolution 23:482–490.

Koch MA. 2019. The plant model system Arabidopsis set in an evolutionary, systematic, and spatio-temporal context. J Exp Bot 70:55–67.

Kopelman NM, Mayzel J, Jakobsson M, Rosenberg NA, Mayrose I. 2015. Clumpak: a program for identifying clustering modes and packaging population structure inferences across K. Mol Ecol Resour 15:1179–1191.

Korneliussen TS, Albrechtsen A, Nielsen R. 2014. ANGSD: Analysis of Next Generation Sequencing Data. BMC Bioinformatics 15:356.

Kremling KAG, Chen S-Y, Su M-H, Lepak NK, Romay MC, Swarts KL, Lu F, Lorant A, Bradbury PJ, Buckler ES. 2018. Dysregulation of expression correlates with rare-allele burden and fitness loss in maize. Nature 555:520–523.

Laenen B, Tedder A, Nowak MD, Toräng P, Wunder J, Wötzel S, Steige KA, Kourmpetis Y, Odong T, Drouzas AD, et al. 2018. Demography and mating system shape the genome-wide impact of purifying selection in *Arabis alpina*. Proceedings of the National Academy of Sciences 115:816–821.

Leinonen PH, Sandring S, Quilot B, Clauss MJ, Mitchell-Olds T, Agren J, Savolainen O. 2009. Local adaptation in European populations of Arabidopsis lyrata (Brassicaceae). American Journal of Botany 96:1129–1137.

Levin DA. 2010. Environment-enhanced self-fertilization: implications for niche shifts in adjacent populations. Journal of Ecology 98:1276–1283.

Lohmueller KE. 2014. The Impact of Population Demography and Selection on the Genetic Architecture of Complex Traits. PLOS Genetics 10:1–16.

Louthan AM, Doak DF, Angert AL. 2015. Where and When do Species Interactions Set Range Limits? Trends in Ecology & Evolution 30:780–792.

Lynch M. 2007. The Origins Of Genome Architecture. 1 edition. Sinauer Associates Inc

Mable BK, Dart AVR, Berardo CD, Witham L. 2005. Breakdown of Self-Incompatibility in the Perennial Arabidopsis Lyrata (brassicaceae) and Its Genetic Consequences. Evolution 59:1437–1448.

Marburger S, Monnahan P, Seear PJ, Martin SH, Koch J, Paajanen P, Bohutínská M, Higgins JD, Schmickl R, Yant L. 2019. Interspecific introgression mediates adaptation to whole genome duplication. Nature Communications 10:1–11.

Marsaglia G, Tsang WW, Wang J. 2003. Evaluating Kolmogorov's Distribution. Journal of Statistical Software 8:1–4.

Mattila TM, Aalto EA, Toivainen T, Niittyvuopio A, Piltonen S, Kuittinen H, Savolainen O. 2016. Selection for population-specific adaptation shaped patterns of variation in the photoperiod pathway genes in Arabidopsis lyrata during post-glacial colonization. Molecular Ecology 25:581–597.

Mattila TM, Tyrmi J, Pyhäjärvi T, Savolainen O. 2017. Genome-Wide Analysis of Colonization History and Concomitant Selection in Arabidopsis lyrata. Mol Biol Evol 34:2665–2677.

Morgan MT, Wilson WG, Knight TM. 2005. Plant Population Dynamics, Pollinator Foraging, and the Selection of Self-Fertilization. The American Naturalist 166:169–183.

Muller M-H, Leppälä J, Savolainen O. 2008. Genome-wide effects of postglacial colonization in Arabidopsis lyrata. Heredity 100:47–58.

Ossowski S, Schneeberger K, Lucas-Lledó JI, Warthmann N, Clark RM, Shaw RG, Weigel D, Lynch M. 2010. The Rate and Molecular Spectrum of Spontaneous Mutations in Arabidopsis thaliana. Science 327:92–94.

Pavlidis P, Živković D, Stamatakis A, Alachiotis N. 2013. SweeD: Likelihood-Based Detection of Selective Sweeps in Thousands of Genomes. Molecular Biology and Evolution 30:2224–2234.

Peischl S, Dupanloup I, Kirkpatrick M, Excoffier L. 2013. On the accumulation of deleterious mutations during range expansions. Molecular Ecology 22:5972–5982.

Peischl S, Kirkpatrick M, Excoffier L. 2015. Expansion Load and the Evolutionary Dynamics of a Species Range. The American Naturalist 185:E81–E93.

Pfeifer B, Wittelsbürger U, Ramos-Onsins SE, Lercher MJ. 2014. PopGenome: An Efficient Swiss Army Knife for Population Genomic Analyses in R. Molecular Biology and Evolution 31:1929–1936.

Pujol B, Zhou S-R, Sanchez Vilas J, Pannell JR. 2009. Reduced inbreeding depression after species range expansion. Proceedings of the National Academy of Sciences 106:15379–15383.

Purcell S, Neale B, Todd-Brown K, Thomas L, Ferreira MAR, Bender D, Maller J, Sklar P, de Bakker PIW, Daly MJ, et al. 2007. PLINK: A Tool Set for Whole-Genome Association and Population-Based Linkage Analyses. The American Journal of Human Genetics 81:559–575.

Pyhäjärvi T, Aalto E, Savolainen O. 2012. Time scales of divergence and speciation among natural populations and subspecies of *Arabidopsis lyrata* (Brassicaceae). American Journal of Botany 99:1314–1322.

Pyhäjärvi T, García-Gil MR, Knürr T, Mikkonen M, Wachowiak W, Savolainen O. 2007. Demographic History Has Influenced Nucleotide Diversity in European Pinus sylvestris Populations. Genetics 177:1713–1724.

Quilot-Turion B, Leppälä J, Leinonen PH, Waldmann P, Savolainen O, Kuittinen H. 2013. Genetic changes in flowering and morphology in response to adaptation to a high-latitude environment in Arabidopsis lyrata. Annals of Botany 111:957–968.

R Core Team. 2018. R: A language and environment for statistical computing. R Foundation for Statistical Computing, Vienna, Austria. Available from: http://www.R-project.org/

Ross-Ibarra J, Wright SI, Foxe JP, Kawabe A, DeRose-Wilson L, Gos G, Charlesworth D, Gaut BS. 2008. Patterns of Polymorphism and Demographic History in Natural Populations of Arabidopsis lyrata.Fay JC, editor. PLoS ONE 3:e2411.

Sandring S, Riihimäki M-A, Savolainen O, Ågren J. 2007. Selection on flowering time and floral display in an alpine and a lowland population of Arabidopsis lyrata. Journal of Evolutionary Biology 20:558–567.

Savolainen O, Lascoux M, Merilä J. 2013. Ecological genomics of local adaptation. Nat Rev Genet 14:807–820.

Schierup MH. 1998. The Number of Self-Incompatibility Alleles in a Finite, Subdivided Population. 149:1153–1162.

Schierup MH, Bechsgaard JS, Christiansen FB. 2008. Selection at Work in Self-Incompatible Arabidopsis lyrata. II. Spatial Distribution of S Haplotypes in Iceland. Genetics 180:1051–1059.

Schierup MH, Mable BK, Awadalla P, Charlesworth D. 2001. Identification and Characterization of a Polymorphic Receptor Kinase Gene Linked to the Self-Incompatibility Locus of Arabidopsis lyrata. :13.

Schmickl R, Jørgensen MH, Brysting AK, Koch MA. 2010. The evolutionary history of the Arabidopsis lyrata complex: a hybrid in the amphi-Beringian area closes a large distribution gap and builds up a genetic barrier. BMC Evolutionary Biology 10:98.

Simons YB, Sella G. 2016. The impact of recent population history on the deleterious mutation load in humans and close evolutionary relatives. Current Opinion in Genetics & Development 41:150–158.

Simons YB, Turchin MC, Pritchard JK, Sella G. 2014. The deleterious mutation load is insensitive to recent population history. Nature Genetics 46:220–224.

Slatkin M. 1995. A measure of population subdivision based on microsatellite allele frequencies. Genetics 139:457–462.

Slatkin M, Excoffier L. 2012. Serial Founder Effects During Range Expansion: A Spatial Analog of Genetic Drift. Genetics 191:171–181.

Sletvold N, Mousset M, Hagenblad J, Hansson B, Ågren J. 2013. Strong Inbreeding Depression in Two Scandinavian Populations of the Self-Incompatible Perennial Herb Arabidopsis Lyrata. Evolution 67:2876–2888.

Stephan W. 2016. Signatures of positive selection: from selective sweeps at individual loci to subtle allele frequency changes in polygenic adaptation. Mol Ecol 25:79–88.

Subramanian A, Tamayo P, Mootha VK, Mukherjee S, Ebert BL, Gillette MA, Paulovich A, Pomeroy SL, Golub TR, Lander ES, et al. 2005. Gene set enrichment analysis: A knowledge-based approach for interpreting genome-wide expression profiles. Proceedings of the National Academy of Sciences 102:15545–15550.

Toivainen T, Pyhäjärvi T, Niittyvuopio A, Savolainen O. 2014. A recent local sweep at the PHYA locus in the Northern European Spiterstulen population of Arabidopsis lyrata. Molecular Ecology 23:1040–1052.

Tsuchimatsu T, Kaiser P, Yew C-L, Bachelier JB, Shimizu KK. 2012. Recent Loss of Self-Incompatibility by Degradation of the Male Component in Allotetraploid Arabidopsis kamchatica.Mauricio R, editor. PLoS Genetics 8:e1002838.

Vekemans X, Poux C, Goubet PM, Castric V. 2014. The evolution of selfing from outcrossing ancestors in Brassicaceae: what have we learned from variation at the *S*- locus? Journal of Evolutionary Biology 27:1372–1385.

Vergeer P, Kunin WE. 2013. Adaptation at range margins: common garden trials and the performance of Arabidopsis lyrata across its northwestern European range. New Phytologist 197:989–1001.

Wakeley J. 1996. The Variance of Pairwise Nucleotide Differences in Two Populations with Migration. Theoretical Population Biology 49:39–57.

Weng M-L, Becker C, Hildebrandt J, Neumann M, Rutter MT, Shaw RG, Weigel D, Fenster CB. 2019. Fine-Grained Analysis of Spontaneous Mutation Spectrum and Frequency in *Arabidopsis thaliana*. Genetics 211:703–714.

Willi Y, Fracassetti M, Zoller S, Van Buskirk J. 2018. Accumulation of Mutational Load at the Edges of a Species Range. Molecular Biology and Evolution 35:781–791.

Willi Y, Griffin P, Van Buskirk J. 2013. Drift load in populations of small size and low density. Heredity 110:296–302.

Wos G, Willi Y. 2018. Genetic differentiation in life history traits and thermal stress performance across a heterogeneous dune landscape in Arabidopsis lyrata. Ann Bot 122:473–484.

Wright SI, Lauga B, Charlesworth D. 2003. Subdivision and haplotype structure in natural populations of Arabidopsis lyrata. Molecular Ecology 12:1247–1263.

Younginger BS, Sirová D, Cruzan MB, Ballhorn DJ. 2017. Is biomass a reliable estimate of plant fitness? Applications in Plant Sciences 5:1600094.

Zhang C, Dong S-S, Xu J-Y, He W-M, Yang T-L. 2018. PopLDdecay: a fast and effective tool for linkage disequilibrium decay analysis based on variant call format files.Schwartz R, editor. Bioinformatics 35:1786–1788.

Table 1: S –locus allelic diversity has been maintained within SP. The number of S-alleles for each population sample, as well as the number of individuals is provided. For each population the allelic richness has been calculated according to a rarefaction protocol with *N*=7.

Population	**S – alleles**	**Allelic Richness**	**Sample Size**
SP	15	7.6	22
PL	14	8.1	17
AUS	10	10.0	7

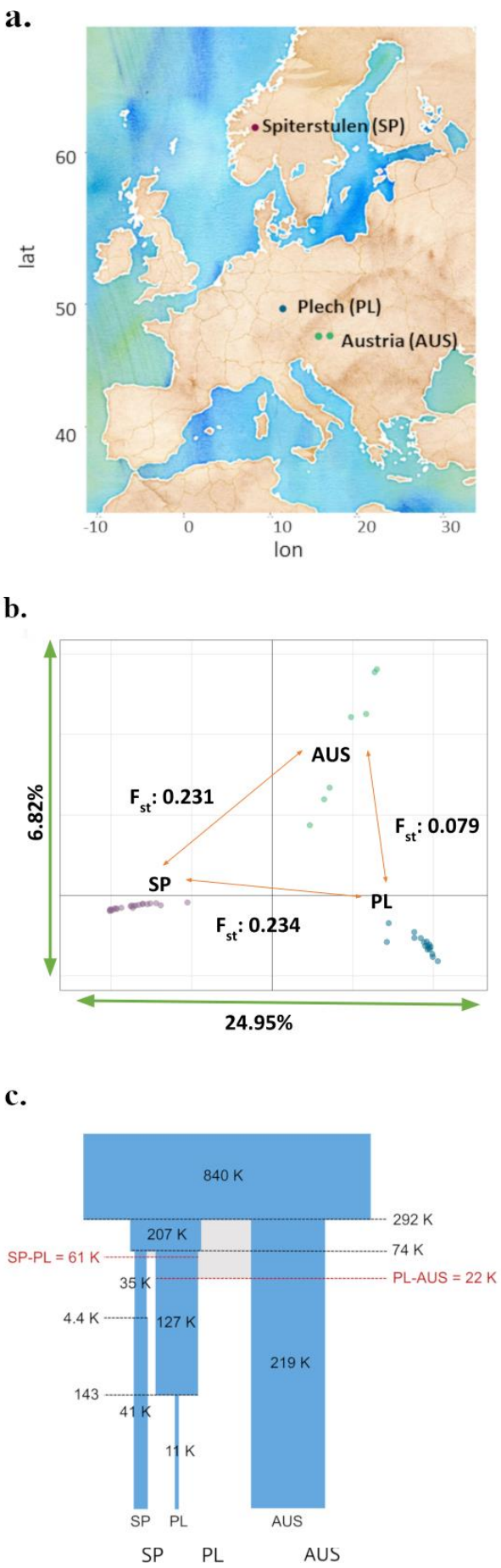

Fig. 1: Population differentiation and demographic analysis of 3 *Arabidopsis lyrata* ssp. *petraea* populations. a. Geographical distribution of the Spiterstulen (SP), Plech (PL) and Austrian (AUS) populations. **b.** Principal Components analysis of SP, PL and AUS. The first Principal Component (PC) explains 24.95% of the sample variation and the second PC explains 6.82%. Within the PCA plot the F_{ST} values between all the population pairs are given. **c.** Schematic representation of the best-fit demography model. Shown within the boxes are the effective number of diploid individuals (Ne), divergence times are indicated with horizontal black lines in thousands of generations and the time since migration ended (horizontal red lines and numbers in red) in thousands of individuals or generations. Width of the elements represents relative differences in Ne, while time-differences in logarithmic-scale are represented by the height of the elements.

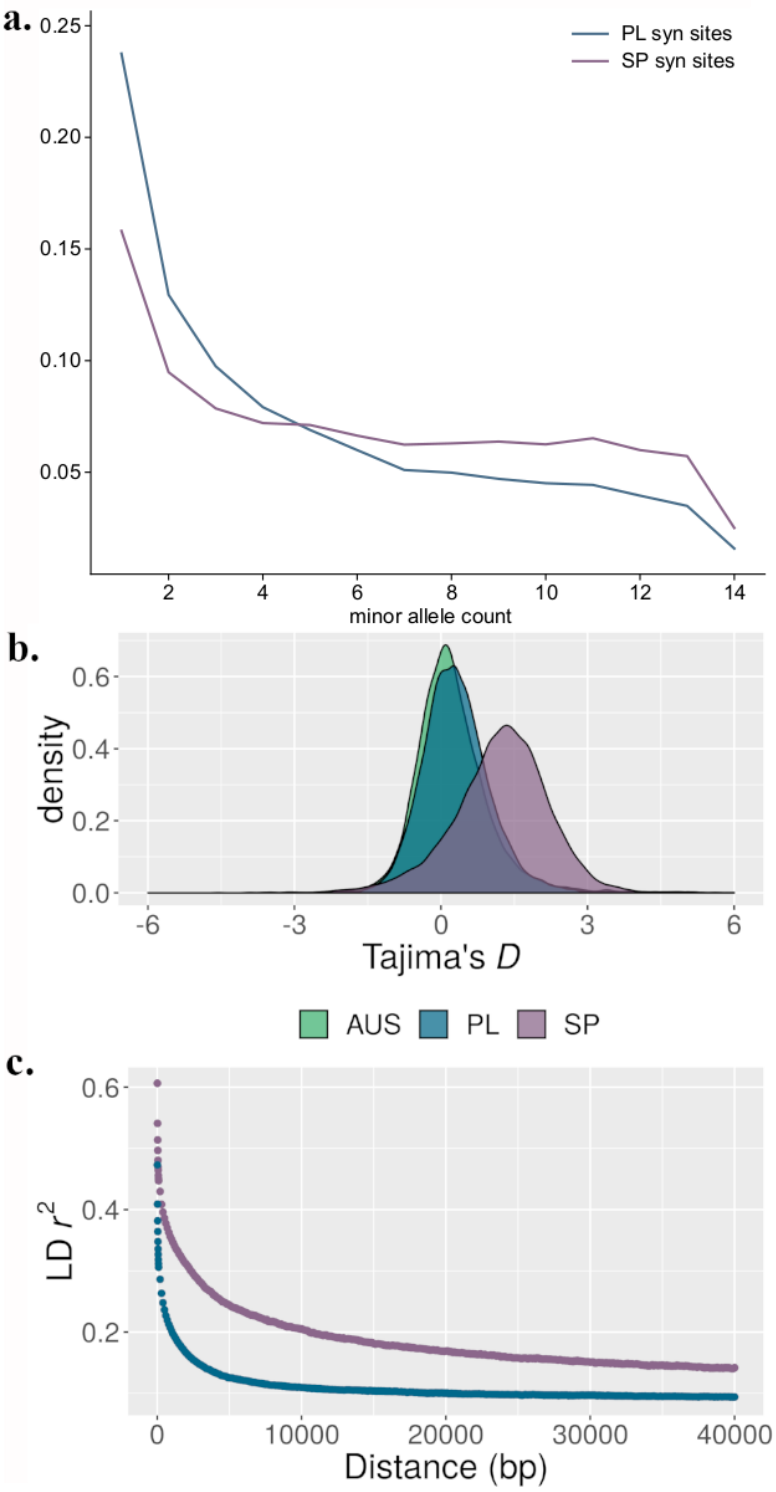

Fig. 2: Evidence of a strong bottleneck along the SP genome. a. Folded site frequency spectrum of synonymous sites for PL and SP **b.** Tajima's D distribution for AUS, PL and SP calculated along the chromosomes in 10kb non-overlapping windows. **c.** Linkage disequilibrium decay in SP and PL given by SNP pairwise r^2 as a function of the distance between the SNPs. For comparison, both populations were down-sampled to 12 individuals each.

Fig. 3: Comparative efficacy of selection and genomic burden in SP and PL. a. ratio of PL/SP of the proportion of variants for each s category and each allele frequency bin. This estimate is based on the gamma distribution of the DFE given by fit∂a∂I and the expected SFS in each category of s. As a proportion of the total number of variants at each count, PL has more slightly neutral and nearly neutral mutations at low frequency and considerably less strongly deleterious mutations. **b.** Difference in per-individual cumulative derived allele burden between PL and SP, based on the contribution of deleterious variants depending on their count in the population assuming the point s estimate of deleterious mutations. Low frequency mutations contribute more to the burden in PL – negative values indicate that an excess of up to 10 000 deleterious mutations with count 10 or less in the population accumulate in each individual in PL-, whereas fixed mutations (count 28 in the population) play an important role in SP. The net difference, given by the end of the line, is 185. **c.** Comparison of genomic load in SP and PL, for synonymous, non-synonymous and high impact mutations. For each population, the genomic load was calculated as the mean number of non-synonymous corrected by the total number of genotyped sites for each sampled individual. The ratio of mean per individual genomic load of SP vs. PL is given. The distribution was established by bootstrap of the genome (see methods).

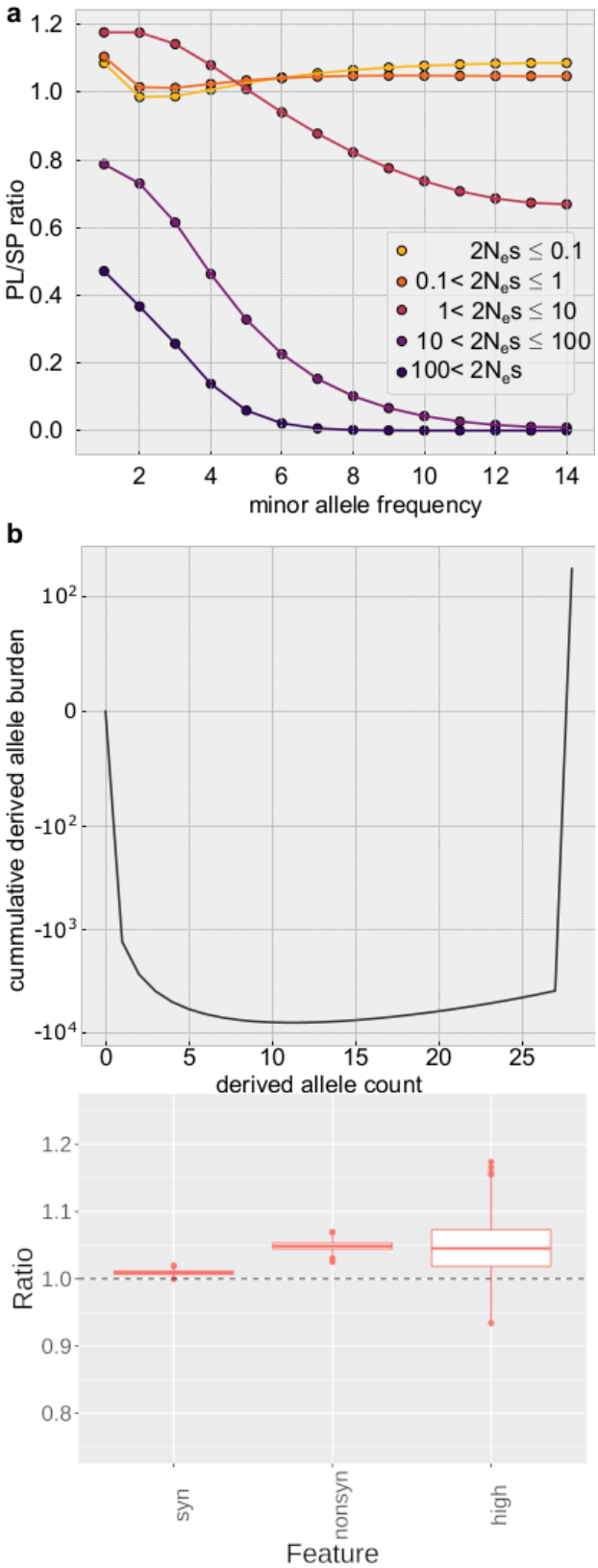

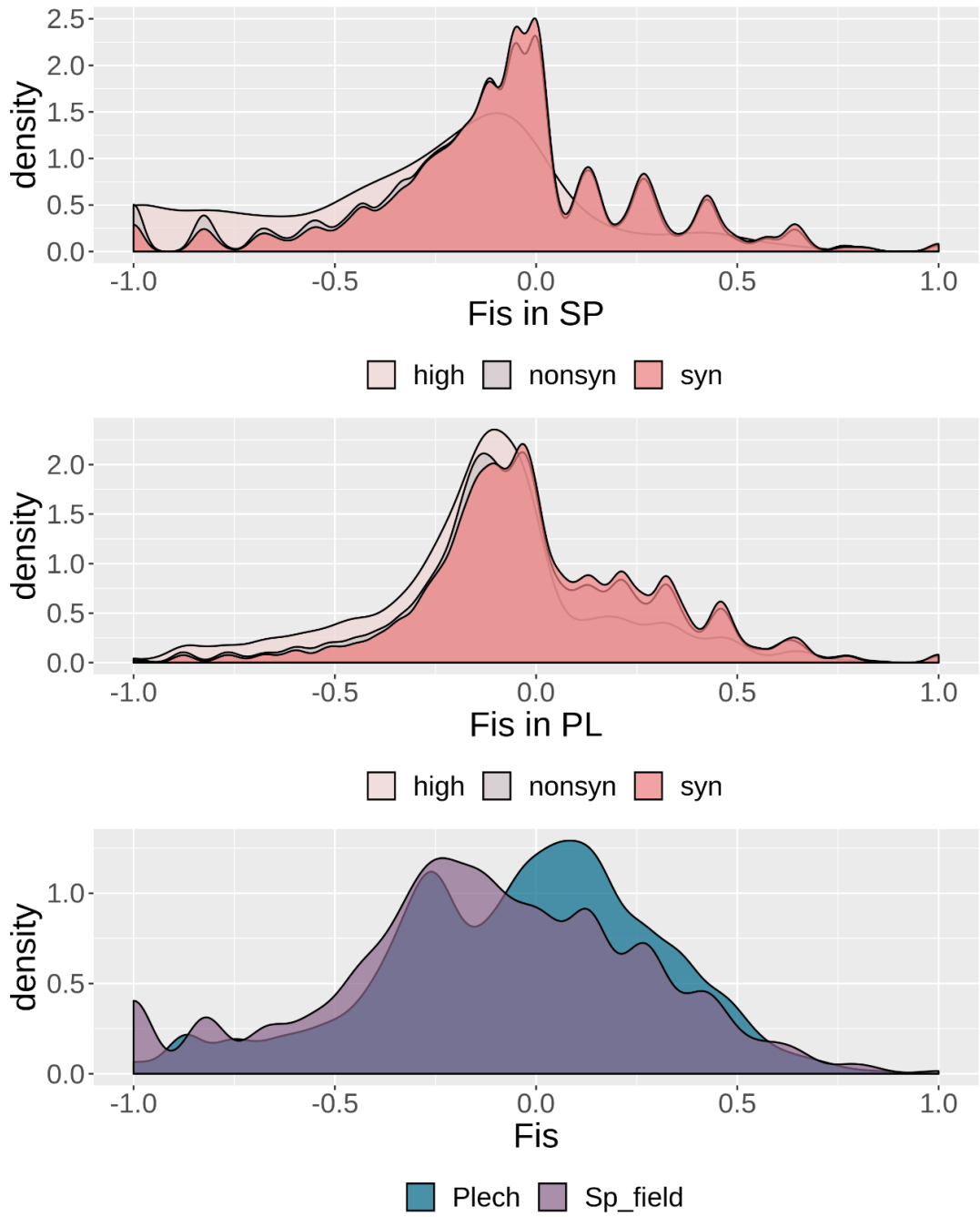

Fig 4: FIS distribution of SP and PL. Top: The FIS of high, non-synonymous and synonymous sites of SP is shown. Middle: The FIS of high, non-synonymous and synonymous sites of PL is shown. Bottom: In blue the FIS distribution for the PL individuals is shown, and in pink the FIS distribution for the field collected SP individuals is provided.